# Density-Functional Study of the Adsorption and Vibration Spectra of Benzene Molecules on Pt(111)

**C. Morin, D. Simon, and P. Sautet***

*Laboratoire de Chimie Théorique et des Matériaux Hybrides, Ecole Normale Supérieure de Lyon, 46 Allée d'Italie, F-69364 Lyon Cedex 07, France, and Institut de Recherches sur la Catalyse, Centre National de la Recherche Scientifique, 2 Avenue Albert Einstein, F-69626 Villeurbanne Cedex, France*

*Received: September 9, 2002; In Final Form: January 24, 2003*

Despite a large number of experimental studies, the adsorption structure of benzene $C_6H_6$ on the (111) surface of platinum is still a matter of debate. In this study, results from first principles Density functional periodic calculations are presented, including the total energy and the simulation of vibrational spectra. Among the six high-symmetry adsorption modes for the molecule, the most stable one corresponds to a bridge site, the C−C bonds in benzene being rotated by 30° with respect to the atomic directions on the surface. The adsorption of the hollow site (rotated by 0°) is less stable by about 0.2 eV. Upon adsorption, the amplitude of the distortion of the molecule and the strength of its interaction with the surface are correlated since they are linked by the variation of the molecular HOMO−LUMO gap. The calculation of the vibrational spectra confirms the total energy results since the bridge structure that is rotated 30° is the only one that is able to reproduce all of the measured bands, and they suggest that the hollow structure could be a minority species. This analysis is consistent with the results obtained from scanning tunneling microscopy, but they contrast with the structure proposed from a low-energy electron diffraction experiment.

## I. Introduction

The transformation of aromatic molecules into less hazardous compounds is today a crucial process for environmental and industrial reasons. Hydrogenation or cracking of these stable molecules can be performed by a transition-metal catalyst. Therefore, an understanding of the interaction between the aromatic molecule and the metal surface can bring important insights to better understand the catalytic mechanisms. Modern first-principle quantum calculations have provided a large amount of knowledge on the chemisorption of small molecules on metal, oxide, or sulfide surfaces. However, despite a large number of experimental studies[1], theoretical calculations on larger molecules such as benzene are not very numerous because of the size of the molecule itself and also because of the surface unit necessary to describe the chemisorption.

In this paper, the adsorption of benzene $C_6H_6$ on a Pt(111) surface is described from first-principle density functional calculations. The choice of this system is clear: benzene is the simplest aromatic molecule, whereas platinum is a major hydrogenation catalyst. Moreover, it has been characterized by several surface science studies. Platinum is indeed very active in the hydrogenation of aromatic molecules, especially benzene.[2,3] The close-packed and stable (111) surface seems to give the largest electronic stabilization.[4]

The first aim of the study was the determination of the adsorption energy and structure of benzene on different sites to foresee the most stable structure. Indeed, the most stable chemisorption structure for benzene on Pt(111) is still a matter of debate since experimental[5−8] and theoretical[9,10] studies yield contrasting conclusions. The second aspect was to understand the nature of the chemical interaction, especially the relation between the molecular distortion and the adsorbate−surface binding process. Finally, the vibrational spectra have been calculated for the various adsorption sites of the molecule to correlate with experimental data.[5,6]

Recent experimental studies using high-resolution electron energy-loss spectroscopy (HREELS), reflection−adsorption infrared spectroscopy (RAIRS), and low-energy electron diffraction (LEED)[5−8,11] have shown that benzene is chemisorbed with its ring parallel to the surface and that the interaction goes through the $\pi$ electrons of the aromatic ring. One difficulty in using the diffraction technique is that the adsorption of benzene on a Pt(111) surface is disordered at the temperature considered (170 K). A periodic ordering can be achieved only by coadsorption with CO ($(2\sqrt{3} \times 4)$rect − $2C_6H_6$ + 4CO structure[7]) or in HF solution ($(\sqrt{21} \times \sqrt{21})R10.9°$ − $3C_6H_6$ structure[12]).

A complex molecule such as benzene can adopt several potential adsorption structures in Pt(111), and the preferred one is still an open question either from experimental or theoretical literature. Figure 1 shows the eight high-symmetry adsorption sites for benzene on Pt(111), classified by the position of the center of mass and the azimuthal angle of the molecule. When coadsorbed with CO in an ordered $(2\sqrt{3} \times 4)$rect − $2C_6H_6$ + 4CO structure, benzene unambiguously adopts a bridge site with the C−C bond rotated 30° from the direction of the Pt rows (bri30 in Figure 1).[7] In the absence of CO, the structure is disordered, and a more difficult diffuse LEED analysis had to be conducted.[8] This suggested as the best candidate the other bridge site (bri0) with a 30° rotation compared to the previous case. The proposed bri0 structure has specific geometric features. First, the Pt−C distances show two very distinct values, with two short Pt−C bonds (2.02 Å) for the two C atoms directly involved in the interaction with the two Pt atoms of the bridge site and four larger ones (2.61 Å) for the remaining ones. Second, a very strong distortion of the benzene molecule appears with C−C distances ranging from 1.45 to 1.63 Å. Such a long

* Corresponding author. E-mail: philippe.sautet@ens-lyon.fr.

10.1021/jp026950j CCC: $25.00 
Published on Web 03/12/2003

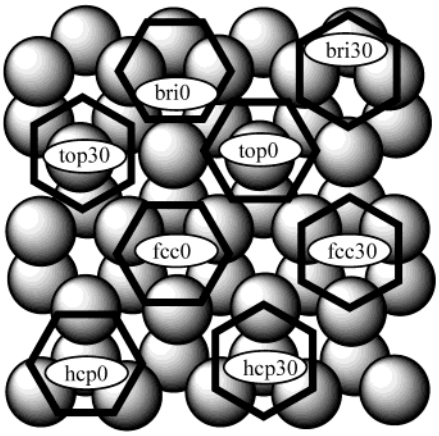


**Figure 1.** High-symmetry adsorption sites of benzene on Pt(111). The hexagon represents the benzene molecule, and the spheres, the Pt atoms.

C−C bond is very unusual for the adsorption of unsaturated molecules on metal surfaces.

Another approach was performed with a vibrational analysis (HREELS) by Lehwald et al.[5] and Cemic et al.,[6] and they concluded that two phases, top0 and hcp0, of benzene exist simultaneously, characterized by different frequency shifts of the CH out-of-plane (830 and 920 $cm^{-1}$) and C−Pt stretching (360 and 570 $cm^{-1}$) modes. Haq et al., after a RAIRS study of benzene adsorbed on Pt(111),[11] proposed that more than one adsorption site is stable, suggesting that a band at 830 $cm^{-1}$ is due to a 3-fold (hcp) adsorption and that a second one at 900 $cm^{-1}$ is due to a 2-fold (bridge) adsorption. The first band is separated into two bands at 830 and 820 $cm^{-1}$ when the temperature increases; these are assigned to the two 3-fold sites (hcp0 and hcp30). Furthermore, a near-edge X-ray absorption spectroscopy (NEXAFS) study[13] concluded that the experimental spectra is correlated to calculated spectra for top0 and top30 adsorption sites, with an estimated cycle−surface distance of 2.6−2.8 Å, but this study did not consider the bridge adsorption sites as possibilities. An angle-resolved UV photoemission (ARUPS) investigation[14] proposed that adsorbed benzene is distorted in a hollow (hcp0 or fcc0) or Kekulé form, with a small magnitude.

Hence, conclusions from spectroscopic techniques are rather confusing. Direct microscopic techniques such as STM can provide very valuable insight on the adsorption sites of molecules. A study performed by Weiss and Eigler[15] showed three different images of adsorbed molecules corresponding to three different adsorption sites: a three-lobed shape, a volcano, and a symmetric bump. When dosing at 4 K and then imaging without warming the crystal, they predominantly found the symmetric bump image and a small proportion of the other two types. When dosing at room temperature and then cooling the crystal before imaging, they observed a ratio of ca. 2:1:3. Under these conditions, the benzene molecules can diffuse across the surface to find energetically favorable sites. A theoretical analysis of these STM images by Sautet and Bocquet[9,16] attributed the different images to molecules adsorbed on hcp0, top0, and bri30 adsorption sites, respectively. The top site is suggested from the experiment to correspond to adsorption at defect sites. Furthermore, image simulation proposes geometry elements for these three modes: the radius is estimated to be 1.5, 1.5, and 1.45 Å, respectively, and the out-of-plane tilt of the H atoms, 20, 20, and 10° respectively.

The problem of the benzene adsorption structure on Pt(111) has also been approached by quantum chemical calculations. Anderson et al., after molecular orbital calculations on benzene coordination to cluster models of the Pt(111) surface,[17] found binding energies of the molecule on different sites at 1.95 eV for bri30, 1.64 eV for hcp0, 1.04 eV for hcp30, 0.74 eV for bri0, and about 0 for the top positions. Despite these results, they concluded that the hcp0 site is the most stable one in relation to an identical study on Ag(111) and Ni(111) that gives hcp0 as the more stable site of adsorption. In an extended-Hückel study, Sautet et al.[18] also found that the most stable chemisorption forms are the hcp0 and bri30 ones with almost identical adsorption energy (∼1.3 eV) and that the top cases are less stable (∼0.9 eV). A study with the same method and a periodic model by Minot et al.[10] confirmed this conclusion, detailed the molecular distortions upon adsorption, and considered the influence of a CO coadsorbate. During the reviewing process of this paper, a very recent theoretical density functional study of benzene adsorption on Pt(111) was brought to our attention. This study mainly uses cluster models with a confirmation on a periodic system.[19]

## II. Methods

Only flat adsorption geometries were considered, and to minimize lateral interactions between neighboring molecules, a $3 \times 3$ unit cell (hence, a $^1/_9$ monolayer coverage) was chosen. Therefore, our study is associated with the low- or medium-coverage adsorption situations, and at high coverage, additional effects could arise from lateral interactions between molecules. Four- and six-layer-thick slabs were used, and the molecule was chemisorbed on the upper face only. In the geometry optimizations, the coordinates of the molecule and two uppermost metallic layers were relaxed. The calculations have been performed with the Vienna ab initio simulation package (VASP).[20,21] This code solves the Kohn−Sham equations of density functional theory using a plane-wave basis set and ultrasoft pseudopotentials[22,23] or the projector augmented-wave method (PAW).[24] The exchange-correlation functional is based on the generalized gradient approximation in the formulation of Perdew−Wang 91. Brillouin-zone integration has been performed using a $5 \times 5 \times 1$ Monkhorst−Pack grid[25] and second-order Methfessel−Paxton smearing[26] with 0.25 eV. The slabs are repeated periodically in the direction perpendicular to the surface, and the vacuum space between neighboring slabs was set to the equivalent of six layers of Pt.

The frequencies and corresponding modes have been calculated by the diagonalization of the Hessian matrix. This matrix has been evaluated by calculating the forces $F_{A,\alpha}^{B,\beta}(\alpha = x, y, z)$ that are exerted on the A atom of the system because of an infinitesimal displacement $d\beta_B$ of the $\beta$ coordinate of the B atom. Then, we approximated

$$\mathrm{Hess}_{A,\alpha}^{B,\beta} = \frac{d^2E}{d\alpha_A d\beta_B}$$

by

$$\mathrm{Hess}_{A,\alpha}^{B,\beta} = \frac{(F_{A,\alpha}^{B,\beta} - F_{A,\alpha}^{B,-\beta})}{2\delta\beta_B}$$

where $\delta\beta_B$ stands for a finite displacement of the $\beta$ coordinate of the B atom. The intensities of the simulated spectra are related to the squared dynamic dipole moment.[27,28] For the *i*th mode,

$$I_i \propto \left| \frac{d\mu}{|d\eta_i|} \right|^2$$

**TABLE 1: Adsorption Energies (eV) of Benzene on a Pt(111) Surface[a]**

| slab[b] | method[c] | *k* points[d] | bri0[e] | bri30[e] | hcp0[e] | hcp30[e] | fcc0[e] | fcc30[e] |
|---|---|---|---|---|---|---|---|---|
| four layers | US (287 eV) | 3*3*1 | −0.26 | −0.80 | −0.55 | −0.30 | −0.53 | −0.31 |
| four layers | PAW (400 eV) | 3*3*1 | −0.27 | −0.87 | −0.62 | −0.31 | −0.59 | −0.30 |
| four layers | PAW (400 eV) | 5*5*1 | −0.30 | −0.90 | −0.67 | −0.33 | −0.61 | −0.27 |
| six layers | PAW (400 eV) | 3*3*1 | −0.66 | −1.27 | −0.97 | −0.61 | | |
| six layers | PAW (400 eV) | 5*5*1 | −0.45 | −1.04 | −0.76 | −0.41 | | |

[a] All calculations correspond to a 3 × 3 surface unit cell. The reference for the energy is the bare surface in the same unit cell and a benzene molecule independently calculated in a 12 × 12 × 12 Å$^3$ box. [b] Number of layers of Pt atoms in the slab. [c] Description of electron−ion interactions (US: ultrasoft pseudopotentials, PAW: projector augmented wave method) and plane-wave energy cutoff for the periodic calculation. [d] *k*-point grid. [e] Adsorption site. (See Figure 1.)

where $d\eta_i$ corresponds to an infinitesimal displacement of the different atoms of the system according to the mode

$$d\eta_i = \sum_{\alpha = x,y,z} \sum_{A=\text{atom}} C^i_{\alpha A} \sqrt{m_A}\, d\alpha_A$$

with, for each mode *i*,

$$\sum_{\alpha,A} (C^i_{\alpha,A})^2 = 1$$

We evaluated $\{d\mu\}/\{|d\eta_i|\}$ as the slope of the function $\mu(x) = \mu(r_0 + x\, d\eta_i)$ (i.e. the variation of the dipole moment when the molecule moves from the equilibrium $r_0$ in the direction of the vibrational mode).

## III. Adsorption Sites

Table 1 presents the calculated adsorption energies for various numbers of layers, K meshes, and choices of pseudopotentiel or plane wave cutoffs. In the case of the four-layer slab, a reasonable energy convergence is achieved for a 3 × 3 × 1 *k*-point grid. This is not, however, the case for the six-layer slab, which requires a finer 5 × 5 × 1 mesh. Tests were constructed on a 7 × 7 × 1 mesh with no significant difference. Once this *k*-point convergence is reached, the six-layer slab consistently gives a slightly more stable adsorption energy by 0.15 eV. Hence, the relative energies between various sites are hardly affected. The change from PAW (cutoff 400 eV) to ultrasoft (cutoff 287 eV) has no significant effect on the adsorption energies, the largest difference being 0.07 eV.

Only six adsorption modes are compared since no stable structure was found when the molecule was positioned on a top site. In the case of the hollow adsorption, the hcp and fcc sites yield very similar results, indicating a negligible influence of the position of the Pt second layer. Hence only one of these structures (hcp) will be described in detail here.

The chemisorption site with the most favorable energy is the bri30 geometry (0.90 eV for the four-layer slab and the PAW method). The second-best case corresponds to a hollow site with the hcp0 and fcc0 configurations (0.67 and 0.61 eV, respectively), but these structures are already 0.23 eV less stable. The other three structures (bri0, hcp30, and fcc30) are significantly higher in energy, and they can be discarded. A recent study by Saeys et al.[19] gives the same trend in the adsorption energies with slightly larger values and an increased difference between the bri30 and hcp0 structures (0.43 eV). This can be attributed to a smaller mesh for Brillouin zone sampling compared to that in our calculations.

The accuracy of GGA DFT calculations for the energy comparison of the molecular chemisorption site on a surface has been recently questioned in the case of CO on Pt(111)[29] and a few other surfaces. Although the agreement between DFT calculations and experiment is excellent for a large number of molecule−surface couples, the case of CO on Pt(111) shed some doubt on the picture. Indeed, the DFT GGA calculation in this case gives the wrong site ordering, with the hollow site favored by 0.10 eV compared to the top site. It is hence not completely clear whether the energy difference of 0.23 eV obtained here in favor of the bri30 geometry is large enough for us to conclude that this geometry is indeed the most favorable one. Hence, we can safely conclude here only that the best configuration is either bri30 or hcp0 (or fcc0).

**TABLE 2: C−Pt Shortest Distances in Different Adsorption Positions**

| site[a] | bri0 | | bri30 | | hcp0 | hcp30 | |
|---|---|---|---|---|---|---|---|
| type[b] | $C_1$−$Pt_1$ | $C_2$−$Pt_4$ | $C_1$−$Pt_1$ | $C_2$−$Pt_4$ | C−Pt | $C_1$−$Pt_1$ | $C_2$−$Pt_1$ |
| occurrence | 2 | 4 | 4 | 2 | 6 | 3 | 6 |
| *d* (Å) | 2.15 | 2.51 | 2.22 | 2.18 | 2.22 | 2.28 | 2.79 |

[a] Adsorption site. (See Figure 1.) [b] See Figure 4 for atom numbering.

Even with such a conservative approach, the theoretical conclusions contrast with the LEED determination, which proposes a bri0 geometry. The bri30 structure also resulted in a very good *R* factor, whereas the final structure refinement was not conducted in the case of the hcp0 geometry. The calculated adsorption energy of the bri0 adsorption is very unfavorable, 0.60 eV less stable than that of the bri30. This structure is hence clearly discarded by the calculation.

## IV. Analysis and Decomposition of Energy

A first crude analysis can be developed in terms of the number of short Pt−C interactions in each structure. All of the values of these short interactions are listed in Table 2. In the most stable geometries (bri30 and hcp0), six Pt−C bonds are formed, whereas only three short bonds are created for the hcp30 and two are created for the bri0, which are the less stable situations.

Another more detailed approach can be proposed by a separation of the various components of the energy. Upon adsorption, the geometry of the molecule and the surface are modified compared to those of the noninteracting systems. This deformation of the system has an energy cost that can be evaluated by a calculation of the energy of the distorted molecule and of the distorted surface separately. However, the distortion favors the interaction between the molecule and the surface, and the interaction energy is calculated as the binding energy between the distorted systems. This energy decomposition scheme is presented for each adsorption structure in Figure 2. The overall adsorption energy appears to be a compromise between an important distortion energy of the molecule (from +0.5 to +1.5 eV) and a large stabilization due to benzene−platinum interaction (from −1 to −2.5 eV). The energetic influence of the surface distortion is more moderate.

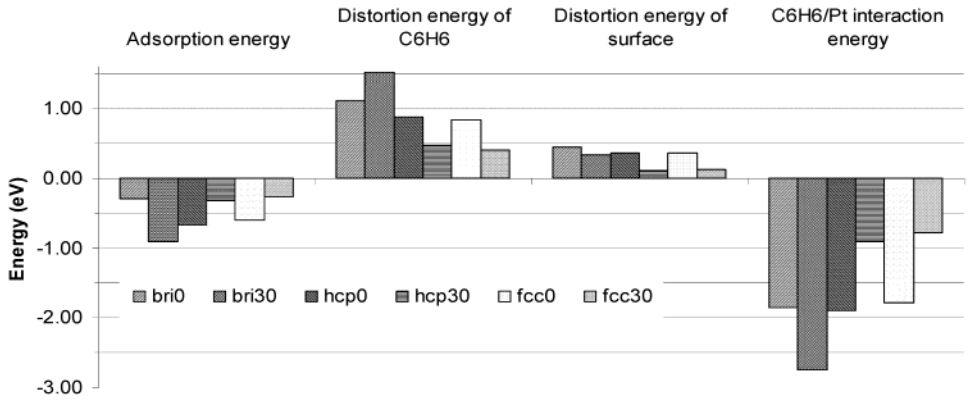


**Figure 2.** Decomposition of the adsorption energy on different sites. The adsorption energy is partitioned into the distortion energy of the surface, the distortion energy of the molecule, and the interaction energy between the molecule and the surface (calculated as the binding energy between the distorted systems).

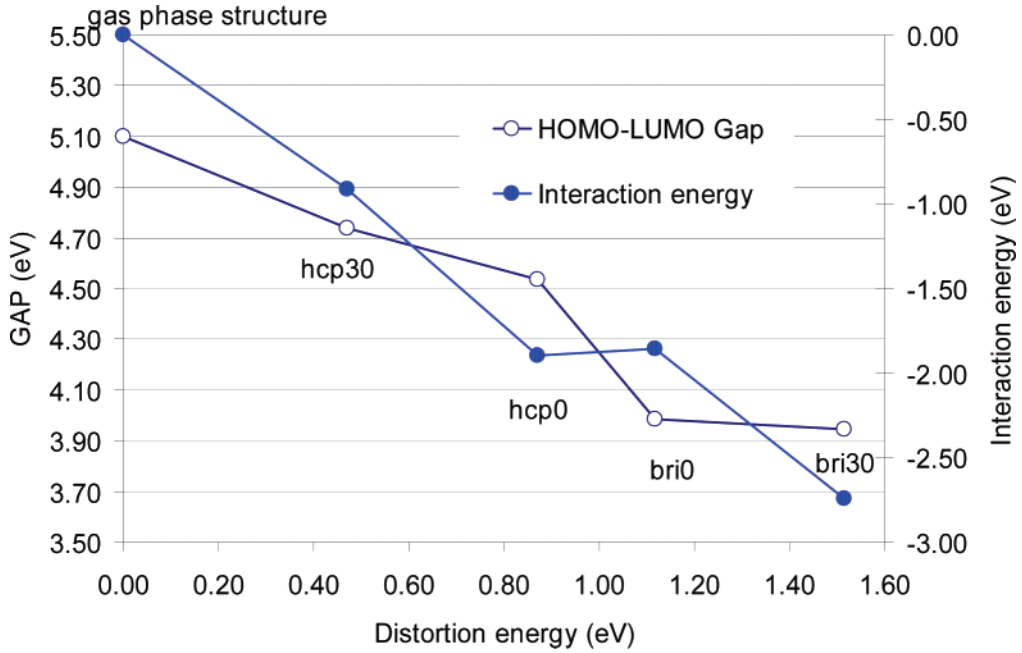


**Figure 3.** (●) Energy gap between the HOMO and LUMO orbitals of isolated benzene in the gas-phase structure and with the distorted geometries of chemisorbed benzene as a function of the molecular distortion energy. (○) Interaction energy between the molecule and the surface.

The bri30 adsorption structure corresponds to the strongest interaction energy but also to the largest distortion cost. Moving to the bri0 orientation markedly decreases the interaction energy (−0.9 eV), whereas the overall distortion cost is weakened by only 0.3 eV, hence explaining the less favorable adsorption energy. The hcp0 (or fcc0) structure corresponds to an interaction energy that is similar to that of bri0, but the distortion energy compromise is much more favorable. Finally, the hcp30 (or fcc30) site gives weak interactions between the molecule and the surface.

It already appears from this analysis that the distortion energy of the molecule and the interaction energy with the surface are linked. This correlation is more clearly shown in Figure 3, the highly distorted molecules (with large distortion energies) having strong interactions with the surface. Upon the distortion of the benzene molecule, the energy and shape of its molecular orbitals are modified. The carbon atoms acquire partial $sp^3$ character, and the $\pi$-orbital overlap in the ring is decreased. The aromaticity of the molecule is partly destroyed. This destabilization of the $\pi$ system is clearly illustrated by the reduction of the HOMO−LUMO gap upon distortion (Figure 3). The distorted molecule then has higher-lying occupied and lower-lying vacant $\pi$ orbitals, which can develop stronger interactions, respectively, with the vacant and filled surface electronic states.

Therefore, the molecular distortion upon adsorption has an electronic origin: it brings the electronic states of the molecule closer to the metal Fermi level, allowing a stronger interaction with the surface. The molecular orbital energy levels play a role, but other aspects such as the spatial overlap between these molecular orbitals and the surface atoms are important. The better overlap, with six short-distance Pt−C contacts, explains the larger interaction energy for bri30 compared to that of bri0, with a similar HOMO−LUMO gap.

## V. Geometry of Adsorbed Molecules

The structural details of the adsorption structures are given in Figure 4 , showing the distortion of the molecule and its position on the surface. Let us start with the most stable structure, bri30. The molecule shows a clear 2-fold distortion, with a slight expansion of its radius from 1.38 Å in the gas phase to an average of 1.45 Å in the surface. The agreement of this radius with the previous determination from STM images calculations[9,16] is very good. The bending of the carbon ring is very moderate, but the out-of-plane displacement of the H atoms

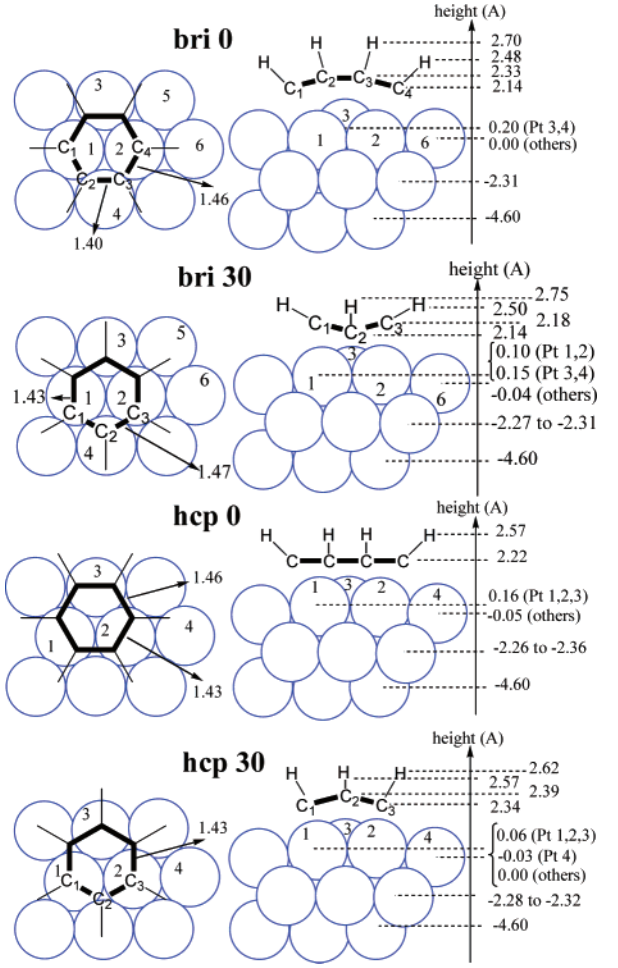


**Figure 4.** Geometry of benzene chemisorbed on Pt(111) for different adsorption sites. Distances are given in angströms. The molecular distortion is exaggerated for clarity.

is significant and different on $C_2$ and $C_3$. The H tilt angles are 37.2 and 15.5°, respectively; each is about half the value associated with full $sp^3$ hybridization. Another important geometric feature is the vertical upshift of the Pt atoms involved in the adsorption by 0.1−0.15 Å. The Pt−C distances are about 2.2 Å (cf. Table 2). Although this bri30 geometry was not the optimum structure in the LEED study, some partial structural results were provided.[8] The Pt−C distance is in good agreement (2.18 Å), whereas the molecular radius is somewhat smaller (1.39 Å) in the LEED structure. The situation is more contrasted for the molecular distortions. The in-plane distortion of the molecule is clear in the calculation with four longer C−C bonds (1.47 Å) and two shorter ones (1.43 Å), but no significant in-plane distortion is shown in the partial LEED data. The out-of-plane distortions are moderate in both cases but are opposite in direction. Another comparison can be performed in the case of the LEED structure determined for the coadsorption of CO and benzene, a case where the adsorption is ordered and where the bri30 structure is the best structure from LEED. The Pt−C distances (2.25 ± 0.05 Å in the experiment) are again in good agreement. The in-plane distortions of benzene are similar this time when theory is compared to experiment. The main difference is in the C−C bond lengths, which are elongated by 0.2−0.3 Å in the experiment compared to those in the calculation. However, the error bar in the experimental determination is large (0.15 Å) in relation to the limited accuracy of LEED for distances in a plane parallel to the surface. The calculated structure is similar to the bridge adsorption obtained for benzene on Ni(111) with DFT[30,31] and for benzene on Pt(111) with extended-Hückel calculations.[10] This structure is also very similar to the one calculated by Saeys et al. in their recent DFT study.[19] Small deviations in bond lengths (0.02 Å for C−C, 0.05 Å for Pt−C) and angles can again be attributed to smaller *k*-point samplings.

Although the bri0 structure is not energetically favorable, the geometry can be compared with that obtained in the diffuse LEED experiment. The ring is distorted with an average C−C distance of 1.44 Å. The bending of the molecule is significant, $C_2$ and $C_3$ and equivalent ones being 0.2 Å higher than the other carbon atoms, and the out-of-plane H bending is similar to that seen before (32.5 and 11.6° for $H_1$ and $H_2$, respectively). Only two carbon atoms ($C_1$ and $C_4$) have short distances with Pt atoms (2.15 Å), the other four having a 2.5-Å distance. This structure is qualitatively similar to that obtained by the diffuse LEED analysis but shows important deviations. The positions of shorter and longer C−C bonds in the ring are inverted, and the experimental values are longer, resulting in a large difference for $d(C_2-C_3)$ (calcd: 1.4 Å; exptl: 1.63 Å). The agreement for Pt−C distances is not good either, with a short Pt−C bond of 2.02 ± 0.02 Å and a long one of 2.61 ± 0.02 Å. Therefore, the energy and geometry both lead us to reject the bri0 structure.

The hcp0, although less stable than the bri30 in the calculation, can, however, reasonably compete. The structure is very symmetrical, all carbon atoms being equivalent with Pt−C distances of 2.22 Å. The average ring radius is 1.445 Å, with a small Kekulé deformation in the ring in relation to the $C_{3v}$ symmetry of the ring. The out-of-plane H tilt is 18.7°, and the three Pt atoms involved in the adsorption are shifted upward by 0.16 Å. Such a hollow chemisorption was proposed for benzene on Pt(111) on the basis of an ARUPS study.[4] This calculated structure is similar to that obtained for benzene on Ni(111).[30]

## VI. Vibrational Study

Because of the contrasting results between our theoretical calculations and the LEED studies, additional information is needed. Vibrational frequencies and intensities for the chemisorbed molecule are clearly important data in bringing complementary insight. As a reference, the vibrational frequencies of gas-phase benzene were first calculated. The obtained values and the experimental ones[32] are listed in Table 3. The different modes are numbered by following ref 33.

The agreement is very good with a maximum difference of ∼2%, without any empirical adjustment of the results. This validates our theoretical approach of vibrational frequencies. For the hard C−H stretching mode, part of the error comes from the neglect of anharmonicity.[34]

HREELS experiments for adsorbed benzene on Pt(111) conclude that the molecule adsorbs parallel to the surface, either in the top0 or hcp0 position,[5] whereas in another study the most probable position is hcp0.[6] A RAIRS study concluded that benzene adsorbs on both hollow and bridge sites.[11] The calculation shows, however, that the top position is not stable, and this leads to eliminate this position. The hcp0 position is found to be the second-most-stable structure after bri30. A detailed theoretical study of the differences in the frequencies spectra may help to assign a preferred site to the experimental data.

The vibrational frequencies calculated for the adsorbed molecule are listed in Table 4 for the four sites that were previously considered. When the losses are observed in the direction of specular reflection, the active modes for high-resolution electron energy-loss spectroscopy belong to the totally

**TABLE 3: Vibrational Frequencies ($cm^{-1}$) of Gas-Phase Benzene**

| mode[a] | $D_6h$ symmetry | description[b] | exptl[c] | computed | error (%) |
|---|---|---|---|---|---|
| $\nu_1$ | $A_{1g}$ | CH str. | 3062 | 3129 | 2.1 |
| $\nu_2$ | $A_{1g}$ | ring str. | 992 | 991 | 0.1 |
| $\nu_3$ | $A_{2g}$ | CH str. | 1326 | 1339 | 1.0 |
| $\nu_4$ | $A_{2u}$ | aop bend | 673 | 666 | 1.1 |
| $\nu_5$ | $B_{1u}$ | aop bend | 3068 | 3090 | 0.7 |
| $\nu_6$ | $B_{1u}$ | ring deform. | 1010 | 997 | 1.3 |
| $\nu_7$ | $B_{2g}$ | aop bend | 995 | 995 | 0.0 |
| $\nu_8$ | $B_{2g}$ | aop bend | 703 | 710 | 1.0 |
| $\nu_9$ | $B_{2u}$ | ring str. + CH bend | 1310 | 1342 | 2.2 |
| $\nu_{10}$ | $B_{2u}$ | ring str. | 1150 | 1143 | 0.6 |
| $\nu_{11}$ | $E_{1g}$ | aop bend | 849 | 842 | 0.8 |
| $\nu_{12}$ | $E_{1u}$ | CH str. | 3063 | 3117 | 1.7 |
| $\nu_{13}$ | $E_{1u}$ | CH bend | 1486 | 1471 | 1.0 |
| $\nu_{14}$ | $E_{1u}$ | ring deform. | 1038 | 1036 | 1.9 |
| $\nu_{15}$ | $E_{2g}$ | CH str. | 3047 | 3102 | 1.8 |
| $\nu_{16}$ | $E_{2g}$ | CH bend | 1596 | 1593 | 0.2 |
| $\nu_{17}$ | $E_{2g}$ | ring deform. | 1178 | 1167 | 0.9 |
| $\nu_{18}$ | $E_{2g}$ | ring deform. | 606 | 600 | 1.0 |
| $\nu_{19}$ | $E_{2u}$ | aop bend | 975 | 962 | 1.4 |
| $\nu_{20}$ | $E_{2u}$ | aop bend | 410 | 405 | 1.2 |

[a] Numerotation of modes from ref 32. [b] str.: streching; bend.: bending; aop: out of plane; deform.: deformation. [c] Experimental values from ref 33.

**TABLE 4: Computed Frequencies of Adsorbed Benzene on Pt(111)**

| | bri0 | | bri30 | | hcp0 | | hcp30 | |
|---|---|---|---|---|---|---|---|---|
| name[a] | $C_2v$[b] | freq. | $C_2v$[b] | freq. | $C_3v$[b] | freq. | $C_3v$[b] | freq. |
| $\nu_1$ | **$A_1$** | **3132** | **$A_1$** | **3103** | **$A_1$** | **3125** | **$A_1$** | **3122** |
| $\nu_2$ | **$A_1$** | **845** | **$A_1$** | **826** | **$A_1$** | **860** | **$A_1$** | **899** |
| $\nu_3$ | $A_2$ | 1296 | $A_2$ | 1296 | $A_2$ | 1310 | $A_2$ | 1310 |
| $\nu_4$ | **$A_1$** | **756** | **$A_1$** | **803** | **$A_1$** | **789** | **$A_1$** | **715−598** |
| $\nu_5$ | $B_1$ | 3073 | $B_2$ | 3050 | $A_2$ | 3099 | **$A_1$** | **3097** |
| $\nu_6$ | $B_1$ | 989 | $B_2$ | 896 | $A_2$ | 893 | **$A_1$** | **986** |
| $\nu_7$ | $B_1$ | 887 | $B_2$ | 990 | $A_2$ | 982 | **$A_1$** | **907** |
| $\nu_8$ | $B_1$ | 620 | $B_2$ | 621 | $A_2$ | 602 | **$A_1$** | **715−598** |
| $\nu_9$ | $B_2$ | 1303 | $B_1$ | 1313 | **$A_1$** | **1345** | $A_2$ | 1348 |
| $\nu_{10}$ | $B_2$ | 1142 | $B_1$ | 1140 | **$A_1$** | **1154** | $A_2$ | 1142 |
| $\nu_{11}$ | $B_1$ | 811 | $B_1$ | 845 | E | 835 | E | 776 |
| | $B_2$ | 779 | $B_2$ | 812 | | | | |
| $\nu_{12}$ | $B_1$ | 3116 | $B_1$ | 3100 | E | 3117 | E | 3115 |
| | $B_2$ | 3122 | $B_2$ | 3090 | | | | |
| $\nu_{13}$ | $B_1$ | 1357 | $B_1$ | 1371 | E | 1381 | E | 1405 |
| | $B_2$ | 1410 | $B_2$ | 1378 | | | | |
| $\nu_{14}$ | $B_1$ | 920 | $B_1$ | 925 | E | 956 | E | 970 |
| | $B_2$ | 952 | $B_2$ | 931 | | | | |
| $\nu_{15}$ | **$A_1$** | **3074** | **$A_1$** | **3042** | E | 3106 | E | 3102 |
| | $A_2$ | 3109 | $A_2$ | 3088 | | | | |
| $\nu_{16}$ | **$A_1$** | **1456** | **$A_1$** | **1430** | E | 1441 | E | 1462 |
| | $A_2$ | 1368 | $A_2$ | 1375 | | | | |
| $\nu_{17}$ | **$A_1$** | **1113** | **$A_1$** | **1134** | E | 1127 | E | 1131 |
| | $A_2$ | 1100 | $A_2$ | 1083 | | | | |
| $\nu_{18}$ | **$A_1$** | **543** | **$A_1$** | **566** | E | 550 | E | 568 |
| | $A_2$ | 556 | $A_2$ | 542 | | | | |
| $\nu_{19}$ | **$A_1$** | **917** | **$A_1$** | **891** | E | 888 | E | 868 |
| | $A_2$ | 870 | $A_2$ | 930 | | | | |
| $\nu_{20}$ | **$A_1$** | **486** | **$A_1$** | **501** | E | 448 | E | 400 |
| | $A_2$ | 406 | $A_2$ | 542 | | | | |
| $\nu_{C-Pt}$ | | 329, 291, 262 | | 358, 352, 327 | | 309, 306, 285 | | 202, 199 |

[a] Name corresponding to the mode of gas-phase molecule except $\nu$C−Pt: mode of largest frequencies concerning C−Pt bonds. [b] Mode symmetry in the symmetry group of the adsorbed molecule. In bold: active mode in specular high resolution of electron energy loss spectroscopy.

symmetric $A_1$ representation of the symmetry point group.[5] Table 4 gives the representations of each mode, and active $A_1$ modes are indicated in bold type. The intensity of each active mode has been computed from the squared dynamic dipole moment, and after a Gaussian broadening of 18 $cm^{-1}$, the simulated spectra are plotted for each adsorption site in Figure 5, together with the experimental data from ref 5. The frequency window has been limited to 1500 $cm^{-1}$, and hence the C−H stretching peak is not shown. The computed frequencies and simulated spectra obtained for bri30 adsorption are in good agreement with those computed by Sayes et al.[19] using a small four-atom cluster to model the surface. Hence, a reduced local model of the surface seems to be adequate for the simulation of vibrational spectra.

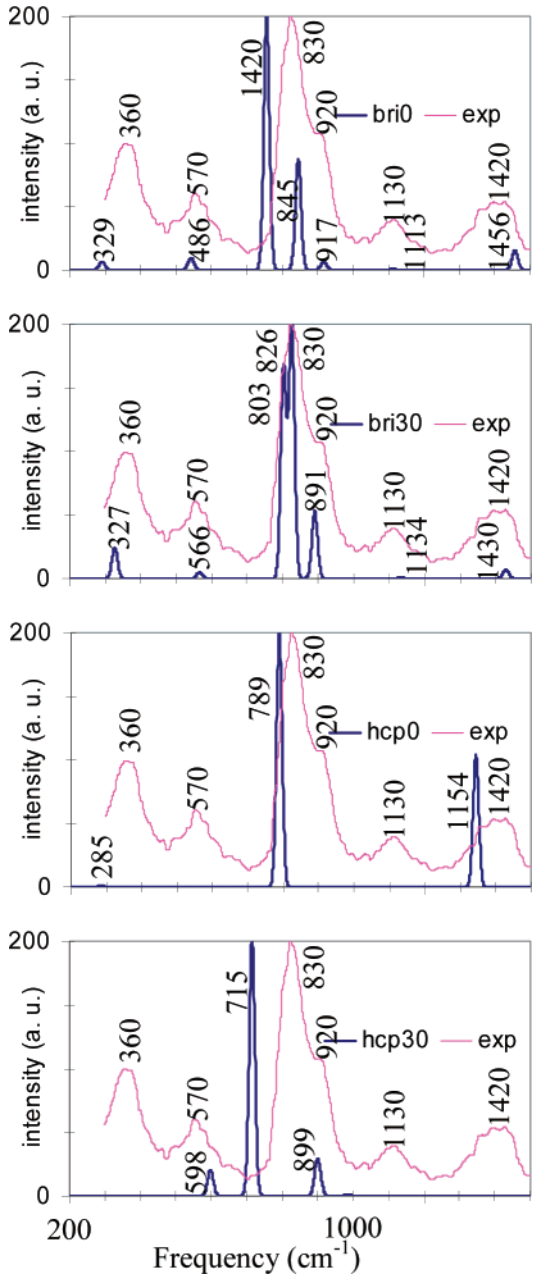


**Figure 5.** Calculated vibrational spectra for benzene chemisorbed on a Pt(111) surface for the four considered adsorption structures with a Gaussian broadening of 18 $cm^{-1}$. These spectra are compared to the experimental HREELS spectrum that is reproduced from ref 5.

As expected, the simulated vibrational spectra of frequencies differ considerably as a function of the adsorption site of the molecule. Moreover, the number of active modes changes when the symmetry of the adsorption site ($C_{2v}$ or $C_{3v}$) or the orientation of the molecule changes. In HREELS experiments,[5,6]

eight different loss features are listed—six well-resolved at 360, 570, 830, 1130, 1410, and 3000 $cm^{-1}$ and two shoulders at 920 and 1310 $cm^{-1}$ (the resolution is ~80 $cm^{-1}$)—and in RAIRS,[11] two bands are observed at 829 and 900 $cm^{-1}$, and a shoulder is observed at 810−820 $cm^{-1}$.

The experimental spectrum is dominated by a high-intensity band at 830 $cm^{-1}$. This loss has been assigned to the symmetric out-of-plane bending of C−H bonds ($\upsilon_4$ mode).[5] All simulated spectra have their most intense band in the 715−826 $cm^{-1}$ interval, but a good frequency match with experiment is obtained only for the bri30 adsorption case, which shows two intense bands at 803 and 826 $cm^{-1}$. These bands are built from a mixing of the out-of-plane bending and ring-stretching modes, both belonging to the same $A_1$ representation of the $C_{2v}$ group. The band at 803 $cm^{-1}$ is moreover associated with a shoulder on the experimental spectra. For the bri0 adsorption, these two bands are more separated (89 $cm^{-1}$), and the most intense band falls in a frequency region (756 $cm^{-1}$) where no band is present in the experiment. The disagreement is also strong for the hcp30 structure with an intense simulated band at 715 $cm^{-1}$, whereas it is more moderated for the hcp0 structure, which shows a single intense band at 789 $cm^{-1}$, which is 40 $cm^{-1}$ away from the measured frequency. (The second band at 860 $cm^{-1}$ has a very small intensity.) Hence, for the most intense part of the spectrum, good agreement is obtained only for the bri30 configuration, which is also the most stable one. This conclusion is amplified only if the smaller-intensity bands are taken into account as described further.

The low-frequency band at 360 $cm^{-1}$ is generally assigned to the vibration of the molecules against the surface.[5,6] This frustrated vertical translation mode of the molecule has a calculated frequency of 327 $cm^{-1}$ and a significant intensity for the bri30 geometry. For the bri0 case, it is shifted to 291 $cm^{-1}$, and hence the agreement is poorer. The same result is obtained for hcp0 with a very weak $\upsilon_{C-Pt}$ mode at 285 $cm^{-1}$, whereas for hcp30 this mode is even softer (~200 $cm^{-1}$).

The second band at 570 $cm^{-1}$ has also been assigned in the literature to the $\upsilon_{C-Pt}$ vibration.[5,6] From the calculation, it is attributed to a ring deformation mode of benzene ($\upsilon_{18}$), which appears at 566 $cm^{-1}$ in the bri30 structure. Its relative intensity is, however, smaller in the calculation than in the experiment, as is the case for all other weak-intensity bands. This band is shifted to 543 $cm^{-1}$ for the bri0 geometry. It does not belong to the $A_1$ representation for the $C_{3v}$ symmetry and hence is not visible for the hcp sites. In contrast, for hcp30, the $\upsilon_8$ out-of-plane bending mode has a nonzero intensity with a frequency of 598 $cm^{-1}$.

The loss at 920 $cm^{-1}$ shown as a shoulder in the experimental spectrum[56] has been the object of two contrasting assignments, either to the $\upsilon_4$ symmetric out-of-plane bending for a different adsorption site of benzene (compared to the intense 830 $cm^{-1}$ band)[5] or to a mixture of $\upsilon_2$ and $\upsilon_{11}$ deformation modes of the molecule.[6] The band at 900 $cm^{-1}$ in the RAIRS study is attributed to a vibration of a molecule on bridge site.[11] From the calculation on the bri30 structure, this rather intense band can be assigned to the $\upsilon_{19}$ out-of-plane bending mode with a frequency of 891 $cm^{-1}$. For the bri0 case, this $\upsilon_{19}$ peak is shifted to 917 $cm^{-1}$, but the intensity is greatly reduced. For hcp0, no band is present in this region, whereas the $\upsilon_2$ ring-stretching mode appears at 899 $cm^{-1}$ for the hcp30 structure. This is a fortuitous agreement, however, and this hcp30 structure has to be clearly discarded from the analysis of other bands.

The loss at 1130 $cm^{-1}$ has been repeatedly assigned to the $\upsilon_{17}$ mode, the only one of gas-phase benzene lying at a similar frequency.[5,6] This is consistent with the calculation for the bri30 adsorption structure, where this ring deformation mode comes at 1134 $cm^{-1}$, and also with the bri0 case (1113 $cm^{-1}$). The calculated intensity is, however, rather small. For the hollow sites, it belongs to the E representation and is hence inactive.

The final peak in the selected window is positioned at 1420 $cm^{-1}$, but it is unusually wide with a shoulder located at 1310 $cm^{-1}$.[6] The main band was assigned to the $\upsilon_{13}$ and $\upsilon_{16}$ modes. $\upsilon_{13}$ is inactive for all adsorption sites, whereas $\upsilon_{16}$ is active for the bridge adsorption cases only, with a frequency of 1430 $cm^{-1}$ for bri30 and 1456 $cm^{-1}$ for bri0. The shoulder at 1310 $cm^{-1}$ has been attributed to the $\upsilon_3$ C−H mode.[6] However, this vibration belongs to the $A_2$ representation for all adsorption structures and is hence inactive in all cases. Another mode of gas-phase benzene, $\upsilon_9$, falls in this frequency range, and it can be described as a combination of ring stretching and C−H bending. This mode is active only for the hcp0 structure, with a high intensity and a frequency of 1345 $cm^{-1}$.

In summary, the adsorption of benzene in the bri30 structures allows us to reproduce and understand all of the measured bands, qualitatively including their relative intensities. This is in good agreement with the favored stability of this structure from the total-energy calculation. However, it does not explain the shoulder at 1310 $cm^{-1}$. In contrast, bri0 and hcp30 conformations can be completely discarded since the calculated vibration with highest intensity clearly falls outside the experimental bands. Moreover, these structures correspond to very unfavorable total energies.

The hcp0 structure is obviously not able to reproduce adequately the complete spectrum, with only two visible bands. It is, however, the only case that is able to provide an active frequency corresponding to the shoulder at 1310 $cm^{-1}$. Considering, from the total energy, that this adsorption geometry is not completely unfavorable, it could be suggested that this hcp0 mode is also present as a minority species (besides bri30). The intensity ratio between the calculated bands at 1456 $cm^{-1}$ for bri30 and at 1345 $cm^{-1}$ for hcp0 indicates as a rough estimation that a ratio of 1 hcp0 to ~25 bri30 molecules could give the observed equivalent intensity for the main peak at 1420 $cm^{-1}$ and its shoulder at 1310 $cm^{-1}$. With such a concentration, the main vibrational band at 789 $cm^{-1}$ for hcp0 would be hidden in the edge of the most intense band of the overall spectrum. It is clear, however, that additional experiments would be necessary to check such a proposal, which is at this point rather speculative. Moreover, the presence and concentration of hcp0 benzene molecules on the Pt(111) surface might depend on the way the sample is prepared.

## VII. Conclusions

The total-energy calculations and the simulation of vibrational spectra lead to a very coherent picture. The bri30 structure is the most stable one, and it is able to reproduce all of the features of the spectrum, except a shoulder at 1310 $cm^{-1}$. The hcp0 geometry (or, equivalently, fcc0) is calculated to be 0.23 eV less stable, and its presence as a minority species on the surface could explain the missing shoulder. The other structures—bri0, hcp30, or top—are clearly excluded for both energy and frequency reasons. The approach also yields an analysis of the nature of the chemical bond between the adsorbate and the surface. It underlines that the molecular distortion upon adsorption is not a consequence of steric repulsion but a way to decrease the energy gap between the HOMO and LUMO orbitals of benzene and hence to control and optimize the strength of the molecule−surface interaction. The chemisorption energy

therefore appears to be a compromise between the cost of molecular distortion and the large stabilization due to benzene−platinum interaction. This process is optimal for the bridge adsorption with the molecule rotated 30° with respect to the atomic lines of the substrate (bri30).

It is interesting that previous results[10,18] from a simple semiempirical method (extended Hückel) agree qualitatively with our results from first principles calculations. The most favored structures (bri30, hcp0) were correctly predicted with the right type of ring distortion. These simple methods yield elegant qualitative analyses from molecular orbitals, but they fail in the precise description of binding energies, distances, and, of course, vibrational spectra.

The benzene molecule has a large number of vibrational modes. To compare with the experimental spectra for such a complex molecule, it is mandatory to go beyond the calculation of frequencies and to evaluate the intensities of the bands in the spectra. This study shows that efficient procedures can be proposed to calculate the intensities from a DFT plane-wave calculation.

The results in terms of the adsorption modes of benzene on platinum are in good agreement with the interpretation of the images obtained with STM.[9,15,16] The symmetric bump, associated with the bri30 structure, is predominant, with a smaller proportion of three-lobed (hcp0 site) or volcano (top site) shapes. The calculation shows that the top site is not stable, but in the experiment, the volcano shape was always associated with a defect on the surface, which could efficiently stabilize it. The agreement is also good with the structure obtained from LEED when benzene is coadsorbed with CO.[7] The bri30 geometry is found, with a good match for the Pt−C distances. Our results, however, clearly disagree with the analysis of the diffuse LEED experiment on pure benzene adsorption.[8] The bri0 structure proposed in this study is in our case discarded from energy, geometry, and vibration calculations. The determination from LEED of a disordered adsorption structure is certainly a more difficult task. The bri30 structure was also considered in the LEED fit procedure, and it also gave a very good *R* factor (0.08 versus 0.05 for the bri0 case). Surface relaxation was not allowed in the fit. Since the Pt atoms involved in the adsorption move upward by 0.1−0.15 Å in our results, the inclusion of surface relaxation could also be important in the LEED fit.

The understanding of the chemisorption properties of benzene on transition-metal surfaces is an important step toward the study of catalytic reactivity processes. It also represents a first approach to the interaction of larger polyaromatic molecules with metal particles, a topic of great interest in the petrochemical industry.

**Acknowledgment.** This work has been supported by the French computational center IDRIS (CNRS), under contract no. 10609. We thank the Center for Computational Materials Science, Materials Physics Institute, University of Vienna for the utilization of the VASP software and for useful discussions.

## References and Notes

(1) Steinrück, H.-P. ; Hubert, W.; Pache, T.; Menzel, D. *Surf. Sci.* **1989**, *218*, 293.
(2) Lin, S. D.; Vannice, M. A. *J. Catal.* **1993**, *143*, 539.
(3) Lin, S. D.; Vannice, M. A. *J. Catal.* **1993**, *143*, 554.
(4) Somers, J.; Bridge, M. E.; Lloyd, D. R.; McCabe, T. *Surf. Sci.* **1987**, *181*, L167.
(5) Lehwald, S.; Ibach, H.; Demuth, J. E. *Surf. Sci.* **1978**, *78*, 577.
(6) Cemic, F.; Dippel, O.; Hasselbrink, E. *Surf. Sci.* **1995**, *342*, 101.
(7) Ogletree, D. F.; Van Hove, M. A.; Somorjai, G. A. *Surf. Sci.* **1987**, *183*, 1.
(8) Wander, A.; Held, G.; Hwang, R. Q.; Blackman, G. S.; Xu, M. L.; de Andres, P.; Van Hove, M. A.; Somorjai, G. A. *Surf. Sci.* **1991**, *249*, 21.
(9) Sautet, P.; Bocquet, M.-L. *Phys. Rev. B* **1996**, *53*, 4910.
(10) Minot, C.; Van Hove, M. A.; Somorjai, G. A. *Surf. Rev. Lett.* **1995**, *3*, 285.
(11) Haq, S.; King, D. A. *J. Phys. Chem.* **1996**, *100*, 16957.
(12) Yau, S.-L.; Kim, Y.-G.; Itaya, K. *J. Am. Chem. Soc.* **1996**, *118*, 7795.
(13) Yimagawa, M.; Fujikawa, T. *Surf. Sci.* **1996**, *357*−*358*, 131−134.
(14) Somers, J.; Bridge, M. E.; Lloyd, D. R.; McCabe, T. *Surf. Sci.* **1987**, *181*, L167−L170.
(15) Weiss, P. S.; Eigler, D. M. *Phys. Rev. Lett.* **1993**, *71*, 3139.
(16) Sautet, P.; Bocquet, M.-L. *Isr. J. Chem.* **1996**, *36*, 63−72.
(17) Anderson, A. B.; McDevitt, M. R.; Urbach, F. L. *Surf. Sci.* **1984**, *146*, 80−92.
(18) Sautet, P.; Bocquet, M.-L. *Surf. Sci.* **1994**, *304*, L445.
(19) Sayes, M.; Reyniers, M.-F.; Marin, B.; Neurock, M. *J. Phys. Chem. B* **2002**, *106*, 7489.
(20) Kresse, G.; Hafner, J. *Phys. Rev. B* **1993**, *47*, C558.
(21) Kresse, G.; Furthmüller, J. *Comput. Mater. Sci.* **1996**, *6*, 15.
(22) Vanderbilt, D. *Phys. Rev. B* **1990**, *41*, 7892.
(23) Kresse, G.; Hafner, J. *J. Phys.: Condens. Matter* **1994**, *6*, 8245.
(24) Kresse, G.; Joubert, D. *Phys. Rev. B* **1999**, *59*, 1758.
(25) Monkhorst, H. J.; Pack, J. D. *Phys. Rev. B* **1976**, *13*, 5188.
(26) Methfessel, M.; Paxton, A. *Phys. Rev. B* **1989**, *40*, 3616.
(27) Person, W. B.; Kubulat, K. *J. Mol. Struct.* **1990**, *224*, 225.
(28) Person, W. B.; Zerbi, G. *Vibrationnal Intensities in Infrared and Raman Spectroscopy*; Elsevier: Amsterdam, 1982.
(29) Feibelman, P. J.; Hammer, B.; Nørskov, J. K.; Wagner, F.; Scheffler, M.; Stumpf, R.; Watwe, R.; Dumesic, J. *J. Phys. Chem. B* **2001**, *105*, 4018.
(30) Mittendorfer, F.; Hafner, J. *Surf. Sci.* **2001**, *472*, 133.
(31) Yamagishi, S.; Jenkins, S. J.; King, D. A. *J. Chem. Phys.* **2001**, *114*, 5765.
(32) Shimanouchi, T. *Tables of Molecular Vibrational Frequencies*; National Bureau of Standards, New York, 1972; Consolidated Vol. 1, pp 1−160.
(33) Herzberg, G. *Molecular Spectra and Molecular Structure II: Infrared and Raman Spectra of Polyatomic Molecules*; Princeton University Press: Princeton, NJ, 1945; p 118.
(34) Cané, E.; Miami, A.; Trombetti, A. *Chem. Phys. Lett.* **2001**, *340*, 356−361.